Cloning and characterization of PDE7B, a cAMP-specific phosphodiesterase

J. M. Hetman*, S. H. Soderling, N. A. Glavas, and J. A. Beavo†

Department of Pharmacology, University of Washington School of Medicine, Seattle, WA 98195

Contributed by J. A. Beavo, October 26, 1999

A member of the phosphodiesterase (PDE)7 family with high affinity and specificity for cAMP has been identified. Based on sequence homologies, we designate this PDE as PDE7B. The full-length cDNA of PDE7B is 2399 bp, and its ORF sequence predicts a protein of 446 amino acids with a molecular mass of 50.1 kDa. Comparison of the predicted protein sequences of PDE7A and PDE7B reveals an identity of 70% in the catalytic domain. Northern blotting indicates that the mRNA of PDE7B is 5.6 kb. It is most highly expressed in pancreas followed by brain, heart, thyroid, skeletal muscle, eye, ovary, submaxillary gland, epididymus, and liver. Recombinant PDE7B protein expressed in a Baculovirus expression system is specific for cAMP with a K_m of 0.03 μM. Within a series of common PDE inhibitors, it is most potently inhibited by 3-isobutyl-1-methylxanthine with an IC_{50} of 2.1 μM. It is also inhibited by papaverine, dipyridamole, and SCH51866 at higher doses. PDE7A and PDE7B exhibit the same general pattern of inhibitor specificity among the several drugs tested. However, differences in IC_{50} for some of the drugs suggest that isozyme selective inhibitors can be developed.

Phosphodiesterases (PDEs) regulate the intracellular levels of cAMP and cGMP. These cyclic nucleotides play an important role as second messengers in multiple physiological processes, including regulation of vascular resistance, cardiac output, visceral motility, immune response, inflammation, neuroplasticity, vision, and reproduction. The great variety of physiological processes regulated by cAMP and cGMP emphasizes the importance of PDEs for the proper function of the organism.

PDEs comprise a large superfamily of enzymes divided into 10 families. Usually, members of the same PDE family show 65% or greater amino acid sequence identity, whereas between families the amino acid identity drops to 40% or lower (1). Different PDEs can be distinguished from each other by their structure, tissue expression, localization, substrate specificity, regulation, and sensitivity to PDE inhibitors. This diversity provides mechanisms for nonoverlapping control of physiological processes by particular members of the PDE superfamily. For example, PDE7A, a cAMP-specific PDE that is expressed in the immune system, has been shown recently to be a critical regulator for the activation of T cells (2). On the other hand, PDE5, a cGMP-specific PDE that is enriched in smooth muscle, is important for control of penile erection (3). This diversity in structure and specificity of function makes PDEs very promising targets for the pharmacotherapy of diseases modulated by cyclic-nucleotide signaling.

Clearly, an important step for understanding the regulation of cyclic nucleotides in normal and disease states is the identification and characterization of the entire PDE superfamily. This would include the cloning of all PDE genes, characterization of their products, and identification of the processes they control. Therefore, we set out to identify, clone, and characterize previously unknown PDEs. To accomplish this task, we took advantage of the public expressed sequence tag (EST) databases (dBEST). Searches of the dBEST EST database for sequences similar to the previously cloned PDE7A resulted in the identification of a murine PDE designated here as PDE7B. In this study, we describe the cloning of the full-length cDNA of this gene, determination of its expression, and characterization of the enzymatic properties of the recombinant PDE7B protein.

Materials and Methods

EST Database Search. The EST database (dBEST) was searched with the published amino acid sequences of mammalian phosphodiesterases. Members of all 10 identified PDE families were used for this search, which was performed with the program BLAST (*B*asic *L*ocal *A*lignment *S*earch *T*ool). All clones identified in the EST database were then used as a query to search GenBank and determine whether they represented known or unknown PDEs. EST clone AI006099 seemed to represent an unknown PDE and was purchased from Genome Systems (St. Louis).

Primers Used. All primers were designed with the program AMPLIFY (freeware by William Engels, Genetics Department, University of Wisconsin, Madison, WI). The primer sequences were: S1, GTGGCGAAGTCTTGTTTGAGAGCCC; AS1, CTGCGGTATAATCCCCCGGAGAAG; S2, GTGTTTGCATGCTAGGAGATGTACGAC; AS2, GCCTAGATGCATGGAAGTATCTTTGG; Strt1, GCTCAGAGATTTCACAGCATTCAAAGG; Strt2, GAACTGCCACTATGGTAAAATGTCTTG; End.1, CATTCTCTTGTATTAAAACTAACAGTATTC; End.2, GGAATCAGTAGCGTTTGGTATTTACAG. All primers were purchased from Operon Technologies (Alameda, CA).

Cloning of the Full-Length cDNA for PDE7B. To obtain the full-length cDNA of PDE7B, the rapid amplification of cDNA ends (RACE) technique was used as described (4). A Marathon-Ready cDNA library from an 11-day-old mouse embryo (CLONTECH) was used as a template. Advantage Polymerase PCR Mix was purchased from CLONTECH. Reactions were carried out as previously described (4).

Sequencing. All PCR products were subcloned into the TA Topo PCRII vector (Invitrogen) according to the manual (Topo TA Cloning, Version E). Plasmid DNA was prepared with the SNAP kit (Invitrogen). Sequencing was done with an ABI PRISM dye terminator cycle sequencing kit (Perkin–Elmer). Sequencing products were purified with Centri-sep columns (Princeton Separations). Sequences were assembled with the program SEQUENCHER 3.0 (Gene Codes, Ann Arbor, MI).

Abbreviations: PDE, phosphodiesterase; RACE, rapid amplification of cDNA ends; EST, expressed sequence tag; IBMX- 3-isobutyl-1-methylxanthine.

Data deposition: The sequence reported in this paper has been deposited in the GenBank database (accession no. AF190639).

*On leave of absence from: Department of Oncology, Centralny Szpital Kliniczny Wojskowej Akademii Medycznej, Szaserow 129, Warsaw, Poland.

†To whom reprint requests should be addressed. E-mail: beavo@u.washington.edu.

The publication costs of this article were defrayed in part by page charge payment. This article must therefore be hereby marked "*advertisement*" in accordance with 18 U.S.C. §1734 solely to indicate this fact.

Northern Blot and RNA Dot Blot Analyses. cDNA clone 12.1.3 encompassing nucleotides 131–441 was used as a probe. Labeling with [α-^{32}P]dCTP (6000 Ci/mmol) was performed with Prime-It RmT random primer labeling kit (Stratagene) followed by purification through Centri-sep columns. Multiple-tissue mRNA Northern blots and mRNA dot blots were purchased from CLONTECH. Prehybridization, hybridization, and washing were done as previously described (4).

Expression of PDE7B and PDE7A. The ORF of the PDE7B cDNA was subcloned into the pFastBac1 baculovirus vector. This vector was electroporated into 1×10^6 Sf-9 cells as described (5). Virus was amplified, and titer was determined by plaque assay (6). To obtain recombinant protein, 1.5×10^8 cells (10^6/ml) were infected at an infection multiplicity of 3 and harvested 3 days later as described (7). Protein extracts were supplemented with 1 vol of glycerol and stored in aliquots at −70°C. In these storage conditions, full activity of PDE7B was maintained for at least 2 mo. Two separate Sf-9 cell infections were done to obtain two independent batches of PDE7B expressing Sf-9 cell homogenates. Human PDE7A (8) was expressed as described for PDE7B.

Kinetics and Inhibitor Studies. PDE assays were carried out according to the method of Hanson and Beavo (9). The reactions were performed in a buffer containing 40 mM Mops (pH 7.5), 0.8 mM EGTA, 15 mM Mg acetate, 0.2 mg/ml BSA, and 50,000 cpm of [^{3}H]cAMP/cGMP. Final reaction volume was 250 μl. The amount of enzyme was adjusted to a level that hydrolyzed no more than 30% of the substrate, even at the lowest substrate concentration tested. For kinetic studies, cAMP/cGMP concentrations varied between 0.1 and 9.2 μM. For inhibitor studies, 12.5 nM and 10 nM cAMP was used for PDE7B and PDE7A, respectively. At such a low concentration of substrate, the IC_{50} approximates the K_i. All kinetic and inhibitor studies were done in triplicate and were repeated three times with homogenates from two independent batches of PDE7B/PDE7A. PDE activity was defined as the difference between activity in Sf-9 cells infected with PDE7B/PDE7A recombinant virus (harvested 3 days post infection) and uninfected Sf-9 cells. 3-Isobutyl-1-methylxanthine (IBMX), *erythro*-9-[3-(2-hydroxynonyl)]adenine, and dipyridamole were obtained from Sigma. Zaprinast was a gift from May & Baker (Dagenham, U.K.). Rolipram was obtained from Biomol (Plymouth Meeting, PA). SCH51866 was a gift from Schering-Plough Research Institute, and sildenafil was a gift from Pfizer Central Research (Sandwich, U.K.). Enoximone was a gift from Merrell Dow Research Institute.

Results

PDE7B Is a Member of the PDE7 Gene Family. The EST database, dBEST, was searched with all published amino acid sequences representing the mammalian PDE superfamily. By using the amino acid sequence of mouse PDE7A as a query, an EST (clone ID AI006099) that was derived from a mouse mammary gland cDNA library was identified. A GenBank search revealed that clone AI006099 was similar but not identical to any of the known PDEs.

EST clone AI006099 was obtained and partially sequenced (463 nt). This EST was clearly a truncated cDNA because both potential translation initiation and stop signals were missing. To obtain the full-length cDNA, we employed RACE reactions. Based on the nucleotide sequence of AI006099, we designed primers S1, S2, AS1, and AS2 for nested 5′- and 3′-RACE reactions. The template for these reactions was a cDNA library prepared from an 11-day-old mouse embryo. Both 5′- and 3′-RACE reactions resulted in multiple clones that were sequenced. Alignment of the nucleotide sequences with the sequenced fragment of EST AI006099 produced a contig that was

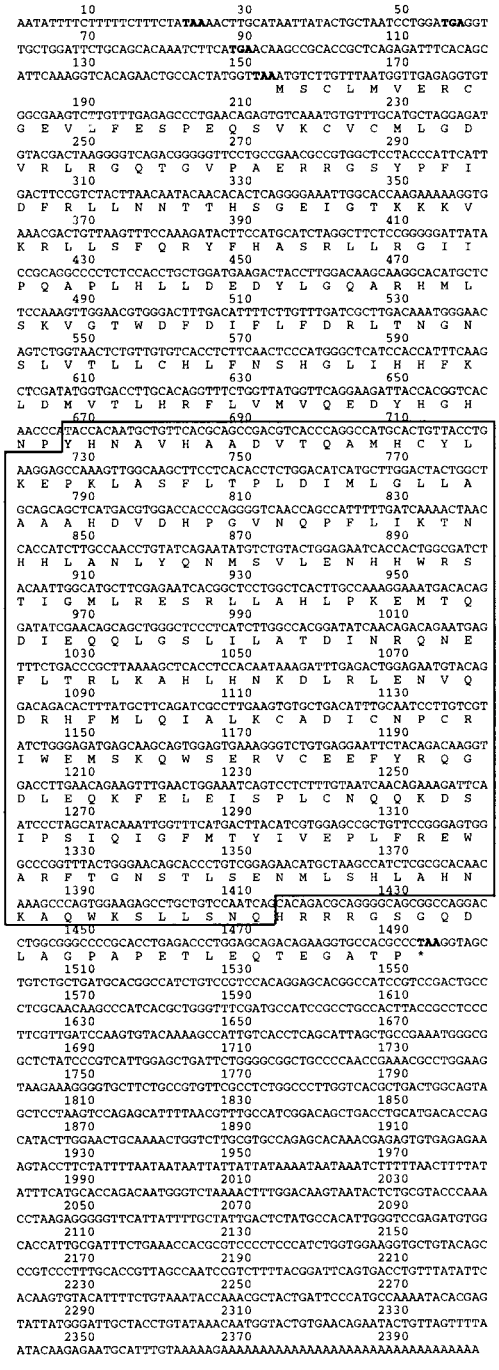

Fig. 1. Nucleotide and amino acid sequence of PDE7B. In- frame stop codons located 5′ to the start methionine are shown in bold. The stop codon at the end of the ORF is shown in bold and marked by an asterisk. The boxed sequence represents the catalytic domain of PDE7B.

1403 bp in length. The contig appeared to include the full 5′ end of the translated coding region, as indicated by the presence of four in-frame stop codons 5′ to the start methionine; however, it did not include the 3′ end.

Further 3′-RACE cloning was carried out with the primers Strt1 and Strt2, the sequences of which were based on the obtained contig sequence. By using these primers, we isolated a clone encompassing the 3′ end of the coding region as revealed by the presence of the poly(A) tail.

To verify cloning results obtained by RACE, we isolated a

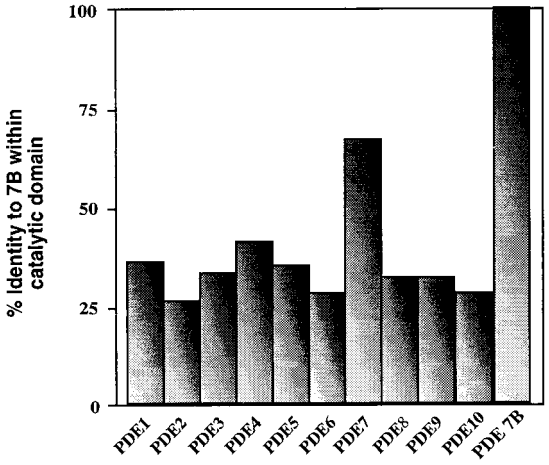

Fig. 2. PDE7B is a member of the PDE7 gene family. The graph depicts the results of an alignment comparing the catalytic domain of PDE7B to the catalytic domains of representatives of the 10 PDE families. The identity between the catalytic domains of PDE7B and PDE7A is 70%, indicating that they are members of the same PDE7 family. Accession numbers for sequences aligned in this figure are: PDE1, L01695; PDE2, U21101; PDE3, Z22867; PDE4, U09457; PDE5, L16545; PDE6, X55968; PDE7, U68171; PDE8, AF067806; PDE9, AF031147; PDE10, AF110507.

single clone containing the full-length cDNA of PDE7B. For this purpose, we designed primers End.1 and End.2, whose sequences mapped just 5′ from the poly(A) tail. These primers were used together with Strt1 and Strt2 primers mapping at the 5′ end of the putative cDNA. Three independent nested PCR were performed with these sets of primers, using the Marathon-Ready cDNA library from an 11-day-old mouse embryo as a template. The resulting clones contained a cDNA with a sequence identical to the contig sequence obtained by alignment of the RACE clones, indicating that a full-length cDNA for this gene had been isolated.

The full-length cDNA is 2399 bp in length, and the ORF predicts a protein of 446 amino acids with a molecular mass of 50.1 kDa (Fig. 1). A consensus PDE catalytic domain is located between nucleotides 667 and 1413. The predicted amino acid sequence of the catalytic domain is 30–40% identical with the catalytic domains of all other PDEs except PDE7A, for which the identity is 70% (Fig. 2). This strongly suggests that the cloned gene represents another member of the PDE7 gene family. We therefore designated this gene as PDE7B.

PDE7B Is Expressed in a Tissue-Specific Manner. To examine the tissue distribution of PDE7B mRNA expression, Northern blot analysis was performed. cDNA clone 12.1.3 (nucleotides 131–441) corresponding to the N terminus of PDE7B was used as a probe. This detected a single band of ≈5.6 kb that is present in heart, brain, liver, and skeletal muscle (Fig. 3*A*). To carry out a more extensive study of the tissue distribution, RNA from 22 different mouse tissues was analyzed by dot blot using the same probe as described above. The dot blot analysis revealed that the message of PDE7B was most abundant in pancreas followed by brain, heart, skeletal muscle, eye, thyroid, ovary, testis, submaxillary gland, epididymus, and liver (Fig. 3*B*). Several other tissues, such as testis, smooth muscle, thymus, prostate, lung, kidney, spleen, uterus, and embryo, had little or no signal, indicating that PDE7B is expressed in a tissue-specific manner and suggesting tissue-specific functions for this enzyme.

PDE7B Is a cAMP-Specific PDE. The ORF of PDE7B was expressed in Sf-9 cells using a Baculovirus expression system. At 0.04 μM

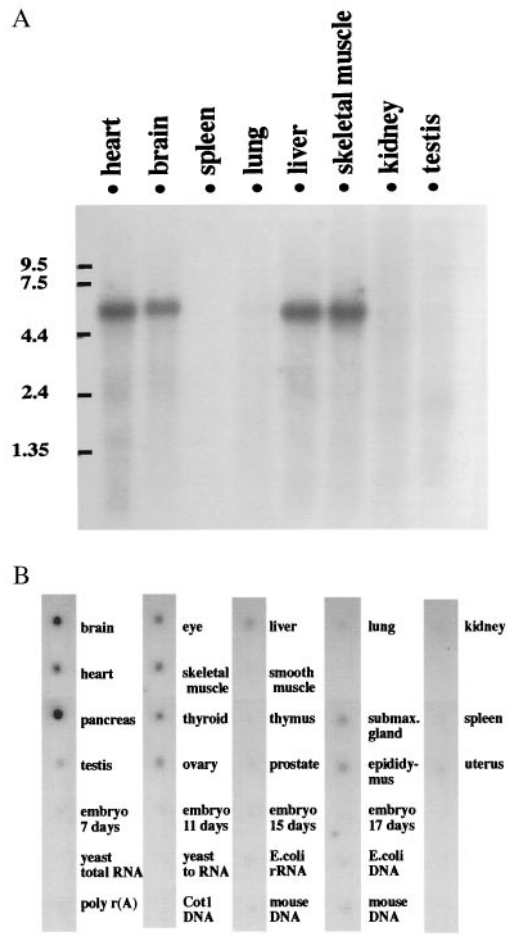

Fig. 3. Tissue-specific expression of PDE7B. (*A*) Northern blot analysis of PDE7B expression. Each lane contained 2 μg of mouse poly(A) RNA. The blot was hybridized with a 310-bp fragment of PDE7B cDNA (nucleotides 131–441). RNA length is indicated by the numbers at the left (kb). A single band, 5.6 kb in size, is present in heart, brain, liver, and skeletal muscle. (*B*) Dot blot analysis of PDE7B expression. Mouse poly(A) RNA dot blots were hybridized as described in *A*. PDE7B message is detected in pancreas, brain, heart, skeletal muscle, eye, thyroid, ovary, testis, submaxillary gland, epididymus, and liver. Please note the strongest signal is in pancreas.

cAMP, extracts from the PDE7B-expressing cells showed a 10-fold increase in cAMP-hydrolyzing PDE activity, as compared with nonexpressing cells. However, no increase in cGMP hydrolysis was observed (data not shown). These findings suggested that PDE7B encoded a cAMP-specific PDE. To further characterize its enzymatic properties, more detailed kinetic studies were performed. The K_m of PDE7B for cAMP was 0.03 μM ($\pm$0.02), as represented by the average of nine separate experiments with two independent enzyme preparations (Fig. 4).

Because there are examples of the regulation of cAMP PDE activity by cGMP (10), we examined effects of cGMP on cAMP hydrolysis catalyzed by PDE7B. Up to concentrations as high as 50 μM, cGMP did not affect the activity of PDE7B (data not shown).

PDE7B Is Sensitive to Several PDE Inhibitors. An obvious approach to start the characterization of the physiological role for PDE7B is to apply specific drugs blocking its activity. Therefore, we set out to determine which, if any, of the several commonly available inhibitors of other PDEs can interfere with the activity of PDE7B expressed in Sf-9 cells. The spectrum of inhibitors tested

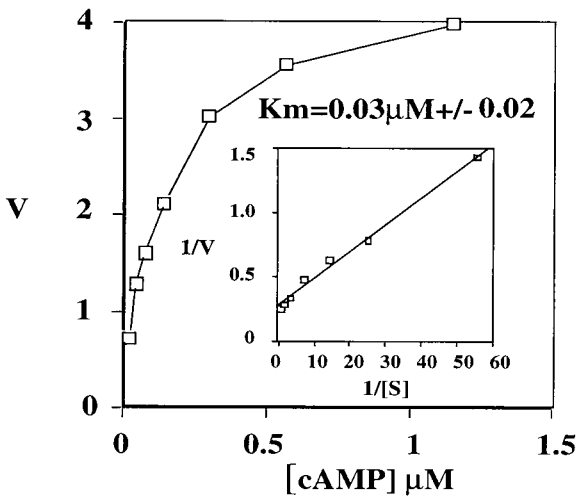

Fig. 4. PDE7B kinetics. The concentration range of cAMP is indicated on the *x*-axis (μM). On the *y*-axis, the velocity (V) of cAMP hydrolysis was plotted (pmol/min/ml). (*Inset*) A Lineweaver–Burk plot of the same set of data. Averages of triplicate determinations in one representative experiment are depicted. The K_m of PDE7B for cAMP was determined to be 0.03 μM ($\pm$0.02) as represented by the average of nine separate experiments with two independent enzyme preparations.

in this study included nonselective compounds as well as selective inhibitors targeting members of other known PDE families. The results of the inhibitor studies are summarized in Table 1. The ability of PDE7B to hydrolyze cAMP was inhibited by IBMX, a nonselective PDE inhibitor. The IC_{50} of IBMX for PDE7B was 2.1 μM. PDE7B was also sensitive to another nonselective inhibitor, papaverine, with an IC_{50} of 22 μM. Dipyridamole, a PDE5, PDE6, PDE8, and PDE10 inhibitor, was also able to inhibit PDE7B with an IC_{50} of 9 μM. SCH51866, a PDE1, PDE5, PDE9, and PDE10 inhibitor, also blocked PDE7B activity with an IC_{50} of 44 μM. Several other inhibitors used in this study (Table 1) did not affect PDE7B hydrolysis of cAMP, even when applied at concentrations exceeding the IC_{50} values for other PDEs by 100-fold.

PDE7 Family Members Have Common Inhibitors. In most cases, members of a specific PDE family can be equivalently inhibited by the same drugs. To determine whether this is the case with the PDE7 family, those compounds identified as inhibitors of PDE7B were tested for their ability to block activity of PDE7A. Recombinant PDE7A was expressed in Sf-9 cells and assayed for its cAMP-hydrolyzing activity in the presence of IBMX, papaverine, dipyridamole, or SCH51866. Each of these drugs also inhibited PDE7A. Inhibition constants (IC_{50}) for these compounds for PDE7A were 4.5, 12.5, 42, and 35 μM, respectively. Thus, PDE7A shows the same general spectrum of inhibitor sensitivity as PDE7B.

Discussion

Searches of the EST database with an amino acid sequence of PDE7A led to the identification and cloning of a cAMP-specific phosphodiesterase. The amino acid identity within the catalytic domains of PDE7A and PDE7B is 70%. Usually PDEs demonstrating 65% or more identity within their catalytic domains are classified as being in the same family. Therefore, the PDE can be classified as PDE7 gene family member PDE7B.

The 2,399-bp cDNA of PDE7B is likely to represent a full-length ORF as it contains four in-frame stop codons 5′ to the start methionine. PDE7B is predicted to be a 446-aa enzyme with a molecular mass of 50.1 kDa. Northern blot analysis shows only one band at 5.6 kb in length. The difference between the cDNA and mRNA size suggests the possibility of larger 5′ and/or 3′ untranslated regions. The predicted sequence length of PDE7B is similar to that of PDE7A1 (482 aa) and PDE7A2 (456 aa).

When expressed in insect cells, PDE7B has PDE activity that is specific for cAMP. The K_m for this activity is 0.03 μM, which is slightly lower than the K_m values reported for PDE7A1 (0.2 μM) and PDE7A2 (0.1 μM) (refs. 8 and 11, respectively). Thus, PDE7B shows high affinity and specificity for cAMP, and this is a common feature of all three identified members of the PDE7 family (see Table 2).

In addition, both recombinant PDE7B and PDE7A were inhibited by the nonselective PDE inhibitors IBMX and papaverine, as well as by the semiselective drugs dipyridamole and SCH51866. For example, dipyridamole, a PDE5, PDE6, PDE8, and PDE10 inhibitor (7), blocked PDE7B with an IC_{50} of 9 μM and PDE7A with an IC_{50} of 42 μM. The 4-fold difference in the IC_{50} value for dipyridamole between PDE7A and PDE7B suggests that more selective compounds that are able to distinguish among PDE7 family members can be made. Other inhibitors tested in this study for effects on PDE7B or PDE7A activity (see Table 1) showed only a poor inhibition, if any. Interestingly, this group included rolipram and Ro-201724, which are specific for PDE4 family members. Thus, sensitivity to these drugs distin-

Table 1. Inhibitor studies of PDE7B expressed in Sf-9 cells

Inhibitor	PDE selectivity IC_{50}	IC_{50} (n = 3) forPDE7B	IC_{50} (n = 3) for PDE7A
IBMX	nonselective (2-50 μM)	2.1 $\pm$ 0.7 μM	4.5 $\pm$ 0.9 μM
Papaverine	nonselective (5-25 μM)	22 $\pm$ 3 μM	12.5 $\pm$ 0.6 μM
EHNA	PDE2 (1 μM)	130 $\pm$ 29 μM	>100 μM
Rolipram	PDE4 (2 μM)	180 $\pm$ 20 μM	>100 μM
Dipyridamole	PDE5 (0.9 μM); PDE6 (0.38 μM); PDE8 (4.5 μM); PDE10 (1.1 μM)	9 $\pm$ 0.9 μM	42 $\pm$ 0.7 μM
SCH51866	PDE1&5 (0.1 μM); PDE9 (1.5 μM); PDE10 (1 μM)	44 $\pm$ 1 μM	35 $\pm$ 1 μM
Enoximone	PDE3 (1 μM)	>100 μM	>100 μM
Sildenafil	PDE5 (3.9 nM)	>390 nM	>390 nM
Ro-201724	PDE4 (2 μM)	>200 μM	>200 μM
Zaprinast	PDE5 (0.76 μM); PDE6 (0.15 μM)	>50 μM	>50 μM
Pentoxifylline	nonselective (45-150 μM)	>200 μM	>100 μM

Conditions for inhibitor studies are described in *Materials and Methods*. EHNA, *erythro*-9-[3-(2-hydroxynonyl)]-adenine.

Table 2. Comparison of PDE7B and PDE7A

	Tissue distribution	Size: mRNA, kb	Size: Protein, aa	Size: Predicted molecular mass, kDA	K_m for cAMP, μM	Inhibitors at IC_{50}, μM*: 1	2	3	4	Function
PDE7A						4.5	12.5	42	35	Activation of T cells in immune response
PDE7A1	Lymphoid tissues, pancreas, placenta, brain, kidney, lung	4.2	482	57	0.2					
PDE7A2	Skeletal muscle, heart	3.8	456	50	0.1					
PDE7B	Pancreas, brain, heart, thyroid, skeletal muscle, eye, ovary, submaxillary gland, epididymus	5.6	446	50.1	0.03	2.1	22	9	44	???

*1, IBMX; 2, papaverine; 3, dipyridamole; 4, SCH51866.

guishes between the PDE4 and PDE7 families, which both share specificity and high affinity for cAMP. Discovery of specific PDE7 inhibitors should be very useful for studies of PDE7 function.

The observation in this manuscript that PDE7A is quite sensitive to IBMX appears to contrast with the report by Ichimura and Kase (12) that the PDE7-like activity they identified from a T cell line was only weakly inhibited by IBMX. Although there might be multiple reasons for this discrepancy, it seems most likely that at the relatively high cAMP concentrations used by this group (1 μM) the concentration of IBMX used was not sufficiently in excess of the substrate. Under such conditions, competitive inhibitors would not effectively compete with cyclic nucleotide and inhibit PDE activity. However, even if this is true *in vitro*, one might expect that IBMX would still be a relatively poor PDE7 inhibitor *in vivo* because the levels of cAMP in most cells stimulated by agonist is likely to be in the μM range. It is also conceivable that PDE7A might not be identical with the activity studied by Ichimura and Kase or that the pharmacological properties of endogenous PDE7A derived from human T cells differs from those of the recombinant PDE7A.

Despite the similarities in the PDE7 family, there are also differences between PDE7B and PDE7A. The diversification between PDE7B and PDE7A is obvious when tissue distribution is compared. PDE7B is highly expressed in pancreas, whereas PDE7A is enriched in lymphoid tissues, suggesting that these enzymes have nonoverlapping, tissue-specific functions.

The physiological roles of the PDE7 family are only beginning to be understood. PDE7A is probably involved in regulating T cell activation during the immune response (2). The role of PDE7B is not known at present; however, the observation that it is highly enriched in the pancreas suggests some involvement in the function of this exocrine and endocrine gland. In addition to PDE7B, there are other PDEs present in pancreas including PDE3, PDE4 (13, 14), and the recently reported PDE1C (15). Because those PDEs were shown to actively participate in the signaling events regulating pancreatic function, it is tempting to speculate that PDE7B also might be engaged in similar regulatory circuits.

In summary, a member of the PDE7 family, PDE7B, has been identified and characterized. Tissue-specific expression suggests tissue-specific functions for this enzyme. Although its physiological role is unresolved at the moment, development of specific inhibitors and antibodies should help uncover these functions.

This work was supported by National Institutes of Health Grants DK21723 and HL60178.

1. Beavo, J. A. (1995) *Physiol. Rev.* **75,** 725–748.
2. Li, L., Yee, C. & Beavo, J. A. (1999) *Science* **283,** 848–851.
3. Boolell, M., Allen, M. J., Ballard, S. A., Gepi-Attee, S., Muirhead, G. J., Naylor, A. M., Osterloh, I. H. & Gingell, C. (1996) *Int. J. Impot. Res.* **8,** 47–52.
4. Soderling, S. H., Bayuga, S. J. & Beavo, J. A. (1998) *J. Biol. Chem.* **273,** 15553–15558.
5. Soderling, S. H., Bayuga, S. J. & Beavo, J. A. (1998) *Proc. Natl. Acad. Sci. USA* **95,** 8991–8996.
6. O'Reilly, D. R., Miller, L. & Luckow, V. A. (1992) *Baculovirus Expression Vectors: A Laboratory Manual* (Freeman, New York).
7. Soderling, S. H., Bayuga, S. J. & Beavo, J. A. (1999) *Proc. Natl. Acad. Sci. USA* **96,** 7071–7076.
8. Michaeli, T., Bloom, T. J., Martins, T., Loughney, K., Ferguson, K., Riggs, M., Rodgers, L., Beavo, J. A. & Wigler, M. (1993) *J. Biol. Chem.* **268,** 12925–12932.
9. Hansen, R. S. & Beavo, J. A. (1982) *Proc. Natl. Acad. Sci. USA* **79,** 2788–2792.
10. Dousa, T. P. (1999) *Kidney Int.* **55,** 29–62.
11. Han, P., Xiaoyan, Z. & Michaeli, T. (1997) *J. Biol. Chem.* **272,** 16152–16157.
12. Ichimura, M. & Kase, H. (1993) *Biochem. Biophys. Res. Commun.* **193,** 985–990.
13. Zhao, A. Z., Zhao, H., Teague, J., Fujimoto, W. & Beavo, J. A. (1997) *Proc. Natl. Acad. Sci. USA* **94,** 3223–3228.
14. Parker, J. C., Van Volkenburg, M. A., Ketchum, R. J., Brayman, K. L. & Andrews, K. M. (1995) *Biochem. Biophys. Res. Commun.* **217,** 916–923.
15. Han, P., Werber, J., Surana, M., Fleischer, N. & Michaeli, T. (1999) *J. Biol. Chem.* **274,** 22337–22344.